QC-06-001 (RP-1311)

Solar Absorption by Each Element in a Glazing/Shading Layer Array

John L. Wright, PhD, PEng
Member ASHRAE

Nathan A. Kotey
Student Member ASHRAE

ABSTRACT

Window solar gain can strongly influence building energy consumption and peak cooling load. Shading devices such as venetian blinds, roller blinds, and drapes are routinely used to control solar gain. There is a strong need for models that allow shading layers to be included in glazing system analysis. This paper presents methods by which existing solar optical models for systems of specular glazing layers can be extended to include the effect of layers that create scattered, specifically diffuse, radiation in reflection and/or transmission. Spatially averaged optical properties (i.e., "effective" optical properties) can be used to characterize shading layers, including their beam-diffuse split. Solution techniques can be formulated on the basis of matrix reduction. However, an alternative technique has been developed with the goal of computational simplicity and speed. These attributes are important in the context of hour-by-hour building energy analysis. Sample calculations are presented.

INTRODUCTION

The presence of glazed area in a building envelope results in solar gain that can strongly influence energy consumption and peak loads. The mechanisms of solar gain and heat transfer through fenestration are well understood, and the use of computer software for the purposes of design, rating, and/or code compliance is common (e.g., UW 1996; Finlayson et al. 1993).

The first step in the thermal analysis of a window is to track the incident solar radiation in order to determine the portions reflected, transmitted, and absorbed as well as the locations of the absorbed quantities. This step is crucial because solar gain generally represents the largest and most widely variable heat gain imposed on the conditioned space. The solar gain of the window frame can safely be ignored in almost all cases (Wright and McGowan 1999). Therefore, a one-dimensional center-glass analysis is customarily used and applied to the view-area of the window.

Shading devices such as venetian blinds, roller blinds, and drapes are routinely used to control solar gain because they can so strongly alter the solar optical properties of the window. Their potential for energy savings is widely recognized (e.g., Chantrasrisalai and Fisher 2004; Collins and Harrison 2004). These devices are also of interest because they can be mechanically operated and therefore have switchable optical properties. Still more energy savings are available because of the possibility of automating the control of shading layers according to a predetermined logic. The recognition of these ideas has raised the need to more carefully quantify the thermal performance of shading devices.

Methods exist for modeling the interaction of incident solar radiation with a glazing system composed of any number of parallel, planar, specular glazing layers. Techniques include ray tracing, net radiation analysis, matrix reduction, and iterative numerical processing. The most noteworthy method is a recursion algorithm devised by Edwards (1977). Edwards' method stands out for many reasons: it is simple, compact, and easily programmed (it can even be applied as a hand calculation); it is computationally fast and efficient; it can be applied to any number of layers; diffuse and/or off-normal beam insolation can be handled; and it does not require the use of matrices or matrix manipulations. Appendix A shows an example of Edwards' method implemented in a Fortran subroutine. Noting the simplicity of this code, it is easy to appreciate the value of Edwards' method.

John L. Wright is a professor and **Nathan A. Kotey** is a student in the Department of Mechanical Engineering, University of Waterloo, Waterloo, Ontario, Canada.

The presence of a shading layer entails added complexity. A portion of the solar radiation that encounters the shading layer will be scattered in some fashion. A full set of bidirectional solar optical properties is required for each layer in the system (Klems and Warner 1995), along with computationally intensive matrix manipulations (Klems 1994a, 1994b), if a high level of detail is required regarding the directional nature of the solar radiation within or leaving the system. This may be the case if daylighting is a high priority.

Often a more practical approach is taken. The research described here is based on the assumption that only specular and/or isotropically diffuse components of solar radiation result from the interaction of insolation with any item in a glazing/shading layer array. An expanded set of solar optical properties is assigned to each layer accordingly. Layers that are not uniform (e.g., venetian blinds, coarse fabric) are assigned spatially averaged, or "effective," solar properties (e.g., Yahoda and Wright 2005; Parmelee and Aubele 1952; Rheault and Bilgen 1989; Rosenfeld et al. 2000; Pfrommer et al. 1996; Farber et al. 1963).

Detailed and simplified glazing/shading multi-layer models will produce results that differ to some extent. It is not clear how serious these differences will be because both methods are in early stages of development and application. No direct and comprehensive comparison has been made. However, use of the beam/diffuse model is in keeping with widespread practice (e.g., Yahoda and Wright 2005; Parmelee and Aubele 1952; Rheault and Bilgen 1989; Rosenfeld et al. 2000; Pfrommer et al. 1996; Farber et al. 1963) and allows for both practicality and generality. Reassurance can be taken specifically from the work of Rosenfeld et al. (2000), which showed good agreement between measured and calculated (beam/diffuse model) solar transmittance and solar gain for a window with a venetian blind—the type of shading layer most likely to produce non-isotropic components of transmitted and reflected solar radiation.

It is worth emphasizing that the method(s) sought in this exercise are intended for use in the context of building energy simulation. This type of computationally intensive, iterative simulation places a strong requirement for speed on any of its submodels. Simplicity is also an important asset because of its inherent connection with speed and because of the desire to offer a model that can be widely and reliably implemented. Both of these requirements favor the use of the more simplified beam/diffuse method of tracking solar radiation.

OBJECTIVE

The goal of this research was to formulate an algorithm that can be used to determine all fluxes of reflected, transmitted, or absorbed solar radiation within a glazing/shading layer array exposed to diffuse and/or beam insolation. Each layer is described by known beam/diffuse solar optical properties. Speed and simplicity were noted to be of high priority.

SOLAR-OPTICAL PROPERTIES

Individual Layers

Consider the interaction of solar radiation with a single layer. The quantities of interest are shown in Figure 1.

A portion of the beam radiation incident at a given layer will leave the layer without being scattered. The solar optical properties associated with this unscattered beam radiation are called *beam-beam properties* and are given the subscript *bb*. More specifically, these properties pertain to beam radiation that is transmitted without change in direction or reflected in a direction consistent with specular reflection from the plane of the layer. The properties needed are front and back reflectances, $\rho_{f,bb}$ and $\rho_{b,bb}$, and front and back transmittances, $\tau_{f,bb}$ and $\tau_{b,bb}$. In the analysis of specular glazing layers, it is recognized that $\tau_{f,bb} = \tau_{b,bb}$. However, this may not be true for shading layers. Figure 2 shows an example, a venetian blind and glazing combination, where it is clear that $\tau_{f,bb} \neq \tau_{b,bb}$ for the venetian blind.

The solar optical properties associated with diffuse radiation, incident on the front or back side of the layer, are $\rho_{f,dd}$, $\rho_{b,dd}$, and τ_{dd}. Diffuse insolation is assumed to produce only diffuse radiation in reflection or transmission at each layer,

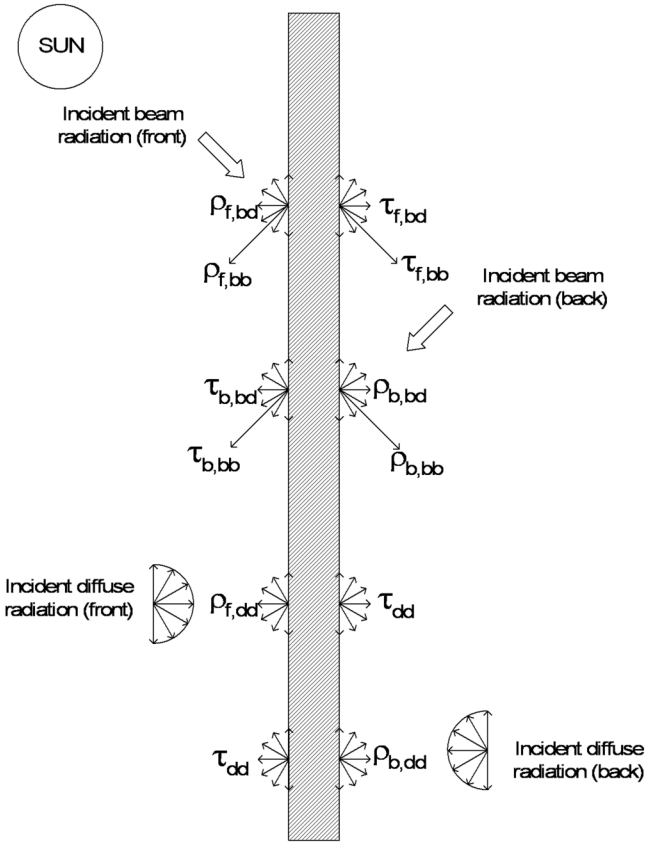

Figure 1 *Solar optical properties of a single glazing or shading layer.*

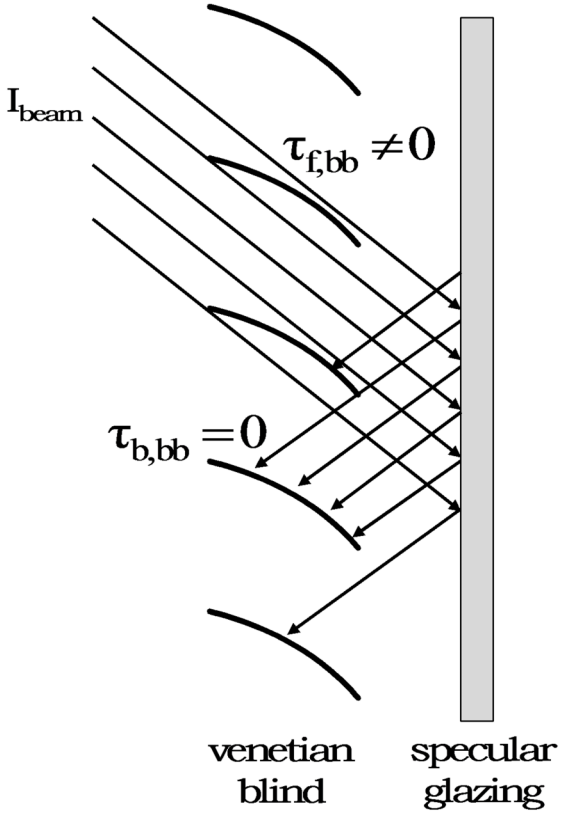

Figure 2 *Example of a shading layer with unequal front and back beam-beam transmittance.*

and the diffuse-diffuse properties are given the subscript *dd*. It can be shown that the diffuse-diffuse transmittance must be the same regardless of whether the incident radiation arrives at the front side or the back side of the layer. Therefore, no *f* or *b* subscript is attached to τ_{dd}.

Beam-beam properties and diffuse-diffuse properties can readily be assigned to specular glazing layers and used to track beam and diffuse insolation, respectively. This is routinely done using Edwards' (1977) method, for example. Added complexity results from the presence of a nonspecular layer because beam radiation can be converted to diffuse radiation. Four additional optical properties are needed: $\rho_{f,bd}$, $\rho_{b,bd}$, $\tau_{f,bd}$, and $\tau_{b,bd}$. The *bd* subscript denotes the beam-diffuse conversion. Again, the front and back transmittance values are not necessarily equal.

Properties of the Environment

In order to fully specify the problem and establish the problem domain, it is useful to assign solar optical properties to the layers that represent the indoor and outdoor environments.

Regarding the outdoor side, it is assumed that none of the radiation leaving the outdoor surface returns. Thus, all reflectance values of the outdoor environment are set to zero. This is quite realistic. No such limitation applies to the reflectance

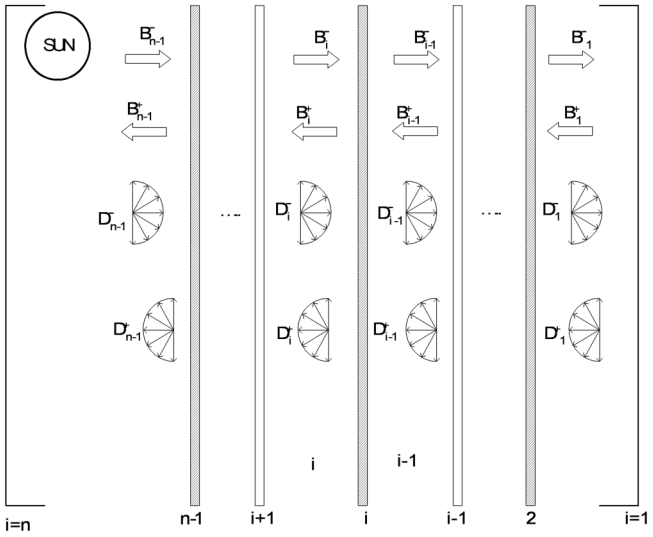

Figure 3 *Beam and diffuse flux components in a glazing/shading layer array.*

of the indoor side. It is also necessary to set the transmittance values to zero for the layers that represent the indoor environment and the outdoor environment.

MODEL AND SOLUTION TECHNIQUE

Solar Flux Components

The multi-layer glazing/shading system is shown in Figure 3. The index *i* is used to indicate location within the system, consisting of layers ranging from $i = 1$ at the indoor space to $i = n$ at the outdoor space. Within the glazing/shading system itself, *i* ranges from $i = 2$ to $i = n - 1$. The solar optical properties of the *i*th layer are illustrated in Figure 1. The gaps are also numbered. The *i*th gap is located between layer *i* and layer $i + 1$.

Figure 3 shows two sets of solar flux quantities, *B* and *D*. The variables B_i^+ and B_i^- are assigned to the indoor-to-outdoor and outdoor-to-indoor fluxes of beam radiation, respectively, in the *i*th gap. The superscript notation and the numbering scheme is consistent with Edwards (1977), allowing for convenient cross-reference.

The beam fluxes are interrelated. Equations 1 and 2 can be obtained by inspection of Figure 3.

$$B_i^+ = \rho_{f,bb,i} B_i^- + \tau_{b,bb,i} B_{i-1}^+ \quad (1)$$

$$B_i^- = \rho_{b,bb,i+1} B_i^+ + \tau_{f,bb,i+1} B_{i+1}^- \quad (2)$$

The *i* (or $i + 1$ or $i - 1$) subscript has been added to the optical properties to indicate the appropriate glazing/shading layer. It is also worth noting that B_{n-1}^- must simply be set equal to the incident flux of beam solar radiation, I_{beam}. B_{n-1}^- is not influenced by B_n^- or B_{n-1}^+, and this is consistent with the

optical properties assigned to the surface that represents the outdoor environment: $\rho_{b,bb,n} = 0$ and $\tau_{f,bb,n} = 0$.

Similarly, D_i^+ and D_i^- are fluxes of diffuse radiation. Note that the incident diffuse flux I_{diff} and D_{n-1}^- are equal. Expressions similar to Equations 1 and 2 can be written for D_i^+ and D_i^- by noting that each diffuse flux arises from both beam and diffuse incident fluxes. These are:

$$D_i^+ = \rho_{f,\,dd,\,i} D_i^- + \tau_{dd,\,i} D_{i-1}^+ + \rho_{f,\,bd,\,i} B_i^- + \tau_{b,\,bd,\,i} B_{i-1}^+ \qquad (3)$$

$$D_i^- = \rho_{b,\,dd,\,i+1} D_i^+ + \tau_{dd,\,i+1} D_{i+1}^- + \rho_{b,\,bd,\,i+1} B_i^+ + \tau_{f,\,bd,\,i+1} B_{i+1}^- \qquad (4)$$

Once all of the B_i^+, B_i^-, D_i^+, and D_i^- values have been determined, it is easy to calculate S_i, the flux of solar radiation absorbed at the ith layer.

$$S_i = B_i^- + B_{i-1}^+ - B_i^+ - B_{i-1}^- + D_i^- + D_{i-1}^+ - D_i^+ - D_{i-1}^- \qquad (5)$$

The flux absorbed at the indoor space and absorbed is S_1.

$$S_1 = B_1^- - B_1^+ + D_1^- - D_1^+ \qquad (6)$$

Matrix Solution

Matrix manipulation can be used to solve for the complete set of solar flux quantities simultaneously. Equations 1 to 4 are applied at each gap from $i = 1$ to $i = n - 1$. Various methods are available to solve the resulting system given by $[L][x] = [R]$, where $[L]$ is the square matrix shown in Figure 4, $[x]$ is a column vector whose transpose is

$$[x]^t = (B_1^-, B_1^+, D_1^-, D_1^+, B_2^-, B_2^+, D_2^-, D_2^+ \ldots B_{n-1}^-, B_{n-1}^+, D_{n-1}^-, D_{n-1}^+)\,, \qquad (7)$$

and $[R]$ is a column vector whose transpose is

$$[R]^t = (0,0,0,0,0,0,0,0,\ \ldots\ 0,0,0,0,\ I_{beam},\ 0,\ I_{diff},\ 0)\,. \qquad (8)$$

Each dimension of $[L]$, $[x]$, and $[R]$ is $n_L = 4(n - 1)$.

Sequential Solution

As an alternative, it is also possible to use a sequential process to obtain the solution for all solar flux quantities. This procedure is based on the ideas that (a) the beam flux values result only from the presence of I_{beam} and are not influenced by diffuse radiation and (b) the diffuse quantities result from the combined influence of I_{diff} and sources of diffuse radiation arising from the interaction of beam radiation with nonspecular layers. This method offers simplicity even to the extent that it can be applied as a hand calculation.

Allowing for the possibility that beam radiation can be converted to diffuse radiation at any given layer, a third set of solar flux variables is defined. The variables C_i^+ and C_i^- describe sources of diffuse radiant flux entering gap i, caused by beam radiation incident at layers i and $i + 1$, respectively (see Figure 5). These beam-diffuse source fluxes are given by Equations 9 and 10.

$$C_i^+ = \rho_{f,\,bd,\,i} B_i^- + \tau_{b,\,bd,\,i} B_{i-1}^+ \qquad (9)$$

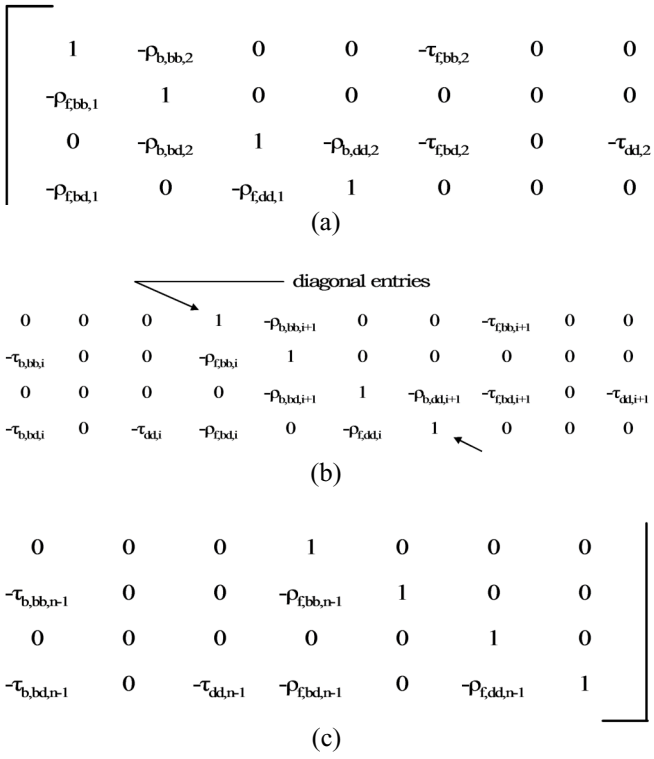

Figure 4 *The* [L] *matrix for simultaneous solution of all beam and diffuse fluxes: (a) upper left corner, (b) general expressions, and (c) lower right corner.*

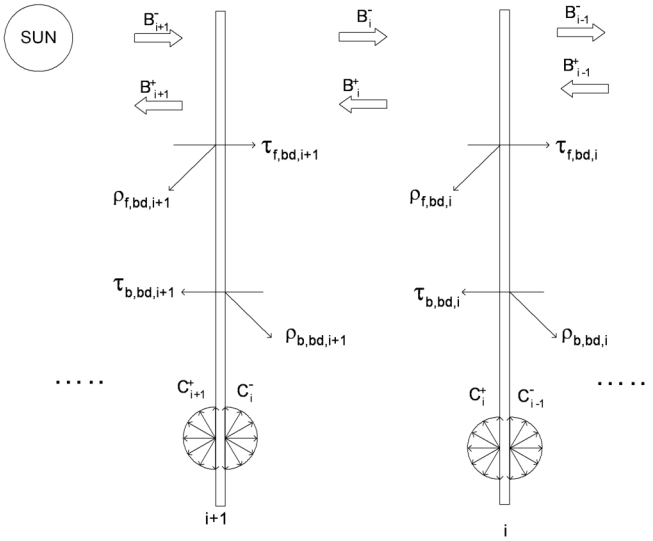

Figure 5 *Sources of diffuse flux caused by beam radiation.*

$$C_i^- = \rho_{b,\,bd,\,i+1} B_i^+ + \tau_{f,\,bd,\,i+1} B_{i+1}^- \quad (10)$$

The sequential solution is undertaken in three steps. First, I_{beam} and the *bb* properties are used to solve for the B_i^+ and B_i^- set. Second, the known values of B_i^+ and B_i^- and the *bd* properties are used to calculate the C_i^+ and C_i^- set. Third, the C_i^+ and C_i^- set along with I_{diff} and the *dd* properties are used to solve for all D_i^+ and D_i^- values. This step is facilitated by recognizing that Equations 9 and 10 can be used to simplify Equations 3 and 4, giving:

$$D_i^+ = \rho_{f,\,dd,\,i} D_i^- + \tau_{dd,\,i} D_{i-1}^+ + C_i^+ \quad (11)$$

$$D_i^- = \rho_{b,\,dd,\,i+1} D_i^+ + \tau_{dd,\,i+1} D_{i+1}^- + C_i^- \quad (12)$$

Step One—Tracking Beam Radiation. Several methods are available to determine the set of B_i^+ and B_i^- values. The Edwards (1977) method is probably the most convenient (see Appendix A). Nonetheless, a different method will be formulated because this technique can most readily be described in the context of the beam-beam radiation problem and then reused in step three to find D_i^+ and D_i^-. Edwards' method is not sufficiently general to include the C_i^+ and C_i^- source terms in the final step.

Applying Equations 1 and 2, it is possible to devise another system of the form [*L*][*x*] = [*R*] that will yield the values of B_i^+ and B_i^-. In this case, [*L*] is the square matrix given in Figure 6 where the *bb* subscripts have been omitted for simplicity, [*x*] is a column vector whose transpose is

$$[x]^t = (B_1^-, B_1^+, B_2^-, B_2^+, \ldots B_{n-2}^-, B_{n-2}^+)\,, \quad (13)$$

and [*R*] is a column vector whose transpose is

$$[R]^t = (0,0,0,0, \ldots 0, -\tau_{f,bb,n-1} I_{beam})\,. \quad (14)$$

Note that the [*L*] matrix shown in Figure 6 has been assembled by applying Equations 1 and 2 to each gap from $i = 1$ to $i = n - 2$. Now $n_L = 2(n - 2)$. The outdoor gap, $i = n - 1$, has not been included. This can be done because, of the two fluxes at the outdoor gap, B_{n-1}^- is known beforehand and B_{n-1}^+ does not influence any of the other fluxes. Therefore, it is sufficient to solve the problem by considering gaps from $i = 1$ to $i = n - 2$ while accounting for the influence of I_{beam} on B_{n-2}^-, which is the function of the last entry in [*R*]. Once this truncated system has been solved, it is possible to finish by using Equation 1 to calculate B_{n-1}^+.

It is important to note that the elements comprising [*x*] have been placed in order such that the only non-zero entries in the [*L*] matrix are found in three lines along the diagonal—a tri-diagonal matrix. This system is easily solved without the use of a matrix. The tri-diagonal matrix algorithm (TDMA), also known as the Thomas algorithm (Thomas 1949; Bruce et al. 1953), is a well-known and well-documented (e.g., Ames 1977) solver applied frequently in computational fluid dynamics. The TDMA is simple, compact, and exceptionally fast. Appendix B shows a TDMA solver written in Fortran. Again, the simplicity of the code is clear.

The TDMA solver operates on a one-dimensional series of unknowns, ϕ_j, associated with nodes from $j = 1$ to $j = m$, as shown in Figure 7. In this application, $m = n_L$. The TDMA solver can be applied if each unknown can be related to its "east" and "west" neighbors, ϕ_{j+1} and ϕ_{j-1}, respectively, in the format of Equation 15. This requirement is satisfied by the tri-diagonal [*L*] matrix.

$$a_j^p \phi_j = a_j^w \phi_{j-1} + a_j^e \phi_{j+1} + b_j^p \quad (15)$$

Once the set of coefficients, a_j^p, a_j^e, a_j^w, and b_j^p, is specified for each node, the TDMA solver generates a solution in a two-pass process. The first pass, from $j = 1$ to $j = m$ (i.e., from west to east), utilizes recursion relations to determine values of α_j and β_j, coefficients used to relate each ϕ_j to its next neighbor to the east, as shown in Equation 16.

$$\begin{bmatrix}
\rho_{f,1} & -1 & 0 & 0 & 0 & 0 & 0 & 0 \\
-1 & \rho_{b,2} & \tau_{f,2} & 0 & 0 & 0 & 0 & 0 \\
\ldots & \ldots & \ldots & \ldots & \ldots & \ldots & \ldots & \ldots \\
0 & 0 & \tau_{b,i} & \rho_{f,i} & -1 & 0 & 0 & 0 \\
0 & 0 & 0 & -1 & \rho_{b,i+1} & \tau_{f,i+1} & 0 & 0 \\
\ldots & \ldots & \ldots & \ldots & \ldots & \ldots & \ldots & \ldots \\
0 & 0 & 0 & 0 & 0 & \tau_{b,n-2} & \rho_{f,n-2} & -1 \\
0 & 0 & 0 & 0 & 0 & 0 & -1 & \rho_{b,n-1}
\end{bmatrix}$$

Figure 6 *The* [L] *matrix for describing a single flux component.*

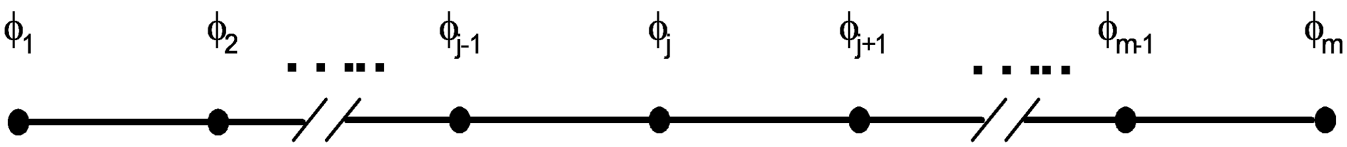

Figure 7 *One-dimensional near-neighbor system solved by the TDMA.*

$$\phi_j = \alpha_j \phi_{j+1} + \beta_j \quad (16)$$

The second pass, from east to west, is used to back-substitute for values of ϕ_j using Equation 16.

The TDMA coefficients can be generated by comparing Equation 15 to the combination of the [*L*] matrix and the [*R*] column vector. The values are assigned as follows, for $i = 1$ to $i = n - 2$:

$j = 2i - 1$

$$a_j^p = \rho_{f,i} \qquad a_j^w = -\tau_{b,i} \qquad a_j^e = 1 \qquad b_j^p = 0 \quad (17a–17d)$$

$j = 2i$

$$a_j^p = \rho_{b,i+1} \qquad a_j^w = 1 \qquad a_j^e = -\tau_{f,i+1} \qquad b_j^p = 0 \quad (18a–18d)$$

Again, the *bb* subscripts have been omitted from Equations 17 and 18 for simplicity.

After all of the coefficient assignments have been made according to Equations 17 and 18, it is necessary to allow for exceptions at $i = 1$ and $i = n - 2$. In order for the TDMA solver to work, the problem domain must be isolated. Specifically, it is necessary to have $a_1^w = 0$ and $a_m^e = 0$. The first condition is satisfied automatically because $\tau_{b,bb,1} = 0$. The second condition requires more scrutiny. Applying Equation 2 at $i = n - 2$ and rearranging in the form of Equation 15,

$$\rho_{b,bb,n-1} B_{n-2}^+ = B_{n-2}^- - \tau_{f,bb,n-1} I_{beam} \ . \quad (19)$$

Noting that $B_{n-2}^+ = \phi_m$ and $B_{n-2}^- = \phi_{m-1}$, it can be seen that the coefficients given by Equation 18 are correct except that a_m^e must be set equal to zero, satisfying the requirement noted above, and the assignment $b_m^p = -\tau_{f,bb,n-1} I_{beam}$ must also be made.

Now execution of the TDMA solver produces the set of B_i^+ and B_i^- values—the individual components of [*x*] being equal to the values of ϕ_j from $j = 1$ to $j = n_L$.

Step Two—Conversion of Beam-to-Diffuse. The C_i^+ and C_i^- values are calculated simply by applying Equations 9 and 10. The most straightforward approach, creating the simplest code, is to step through the layers from $i = 2$ to $i = n - 1$ applying Equation 9 and a modified form of Equation 10:

$$C_{i-1}^- = \rho_{b,bd,i} B_{i-1}^+ + \tau_{f,bd,i} B_i^- \quad (20)$$

Complete the set with C_1^+. An attempt to apply Equation 9 at $i = 1$ will fail because B_0^+ is undefined. A modified form of Equation 9 can be used:

$$C_1^+ = \rho_{f,bd,1} B_1^- \quad (21)$$

It is not necessary to evaluate C_{n-1}^-.

Step Three—Tracking Diffuse Radiation. The D_i^+ and D_i^- set is found by applying Equations 11 and 12 to obtain a system of the form [*L*][*x*] = [*R*]. The [*L*] matrix is unchanged, as given in Figure 6, except that in this case (a) the *dd* solar optical properties must be used instead of the *bb* properties, (b) the restriction that $\tau_{f,dd,i} = \tau_{b,dd,i} = \tau_{dd,i}$ applies, and (c) the *B* entries in [*x*] must be replaced by the corresponding *D* variables.

$$[x]^t = (D_1^-, D_1^+, D_2^-, D_2^+, \ldots D_{n-2}^-, D_{n-2}^+) \quad (22)$$

The most prominent change is in the right-hand-side vector, [*R*].

$$[R]^t = (-C_1^+, -C_1^-, -C_2^+, -C_2^-, \ldots -C_{n-2}^+, -(\tau_{dd,n-1} I_{diff} + C_{n-2}^-)) \quad (23)$$

The general assignment of TDMA coefficients, given by Equations 17 and 18, remains unchanged except that *dd* properties are now used and the b^p coefficients must match revised entries in [*R*].

$$b_j^p = -C_i^+ \qquad j = 2i - 1 \quad (24)$$

$$b_j^p = -C_i^- \qquad j = 2i \quad (25)$$

Exceptions are $a_1^w = 0$, $a_m^e = 0$, and $b_m^p = -(\tau_{dd,n-1} I_{diff} + C_{n-2}^-)$.

In this case the TDMA solver assigns values for D_i^+ and D_i^- from $j = 1$ to $j = n_L$. The procedure is completed by calculating D_{n-1}^+ using Equation 11.

Special Considerations

An error will occur (division by zero) if the TDMA coefficients include $a_1^p = 0$. This appears to preclude the possibility of setting $\rho_{f,bb,1} = 0$ or $\rho_{f,dd,1} = 0$, both of which are routinely used. The problem is easily remedied by using a reverse-TDMA solver. That is, it is possible to execute an east-west sweep followed by a west-east sweep instead of the more traditional west-east/east-west sequence. However, the reverse-TDMA cannot tolerate $a_m^p = 0$. In this case, it is not possible to use $\rho_{b,bb,n-2} = 0$ or $\rho_{b,dd,n-2} = 0$. The latter should never occur. No layer will reflect none of the incident diffuse radiation. The former restriction also appears to be extremely unlikely, but it is possible that some nonspecular layer will be treated as "purely diffuse" and treated as though 100% of the incident beam radiation will be reflected as diffuse radiation. For example, an insect screen located on the outdoor side of the window could trigger this problem. Two remedies are available: (1) Be careful to assign at least some very small amount of beam-beam reflectance to the indoor-facing side of the outdoor layer (say $\rho_{b,bb,n-2} = 0.0001$) or (2) simply use the modified version of Edwards' (1977) method shown in Appendix A to solve for the B_i^+ and B_i^- fluxes.

Insolation on the Indoor Side

The TDMA solution of the D_i^+ and D_i^- fluxes is sufficiently general that it offers an interesting by-product. In addition to I_{beam} and I_{diff} it is possible to specify a third flux of

incident solar radiation, say I_{ind}, that is a diffuse flux incident on the indoor side of the window. The source could be other windows or indoor lighting. This feature might be used to help quantify the time-wise cooling load caused by a step input of heat gain associated with lighting in a specific building.

The procedure is to simply augment the flux of diffuse radiation from the indoor surface, C_i^+. Specifically, an exception to Equation 24 is used:

$$b_1^p = -(C_1^+ + I_{ind}) \tag{26}$$

This method of lumping I_{ind} with C_i^+ is convenient, but other adjustments must be made. Equation 6 will no longer be valid. Even though I_{ind} should not be treated as energy originating at node 1, this will automatically happen because I_{ind} is implicitly included as a component of D_i^+. Suitable replacements for Equation 6 are:

$$S_1 = B_1^- - B_1^+ + D_1^- - (D_1^+ - I_{ind}) \tag{27}$$

$$S_1 = (1 - \rho_{f,bb,1} - \rho_{f,bd,1})B_1^- + (1 - \rho_{f,dd,1})D_1^- \tag{28}$$

The portion of incident solar radiation absorbed at node i, A_i, can now be expressed in a general manner.

$$A_i = \frac{S_i}{I_{beam} + I_{diff} + I_{ind}} \tag{29}$$

EXAMPLES

Consider a multi-layer system with the following elements: an insect screen on the outdoor side and a double-glazed window and a venetian blind on the indoor side. Beam and diffuse solar radiation are simultaneously incident with beam radiation at an angle of 30 degrees from normal. Table 1 summarizes the solar optical properties used in the calculation. The solar properties of the insect screen were estimated from measurements of diffuse-plus-specular (actually normal hemispheric) properties using a Varian Cary 5000 UV/VIS/NIR spectrophotometer. It should be noted that optical properties of the insect screen are approximate, as the measurements were made at normal incidence. Furthermore, the beam-diffuse split and the diffuse properties were coarse estimates based on judgement. The solar optical properties of the glass layers were calculated from the knowledge of the thickness, the refractive index, and the extinction coefficient. The solar optical properties of the venetian blind were calculated using the models of Yahoda and Wright (2005). In calculating the solar optical properties of the venetian blind, a profile angle for beam solar radiation of five degrees was used. Finally, the solar optical properties of the indoor space were set to reasonable, but arbitrary, values.

Table 1. Solar Optical Properties of Glazing/Shading Layers Used in Example Calculations (Incidence Angle 30°, Profile Angle 5°, Slat Angle 50°)

Solar Property	Insect Screen	Glass	Venetian Blind	Indoor Space
$\rho_{f,bb}$	0.000	0.080	0.021	0.048
$\rho_{b,bb}$	0.000	0.080	0.008	0.000
$\rho_{f,bd}$	0.052	0.000	0.499	0.002
$\rho_{b,bd}$	0.052	0.000	0.479	0.000
$\rho_{f,dd}$	0.059	0.140	0.428	0.060
$\rho_{b,dd}$	0.059	0.140	0.478	0.000
$\tau_{f,bb}$	0.750	0.830	0.019	0.000
$\tau_{b,bb}$	0.750	0.830	0.154	0.000
$\tau_{f,bd}$	0.076	0.000	0.206	0.000
$\tau_{b,bd}$	0.076	0.000	0.196	0.000
τ_{dd}	0.650	0.760	0.384	0.000

In the first example, the layers of the system are arranged as shown in Figure 8. The insect screen is on the left and the venetian blind is on the right. The solution was obtained using beam flux $I_{beam} = B_{n-1}^- = 600$ W/m^2 and diffuse flux $I_{diff} = D_{n-1}^- = 75$ W/m^2 (and $I_{ind} = 0$). Figure 8 shows that 16% of the solar radiation is absorbed at the indoor space, 15% by the venetian blind, 10% by the indoor glass layer, 15% by the outdoor glass layer, and 17% by the insect screen. The remaining portion, 27%, is reflected to the outdoor environment. The fluxes of diffuse radiation due to beam radiation, the C sources, can be found at the nonspecular surfaces.

In the second example, as shown in Figure 9, the insect screen is removed from the system. All else remains unchanged. Figure 9 shows that for this arrangement, 19% of the solar radiation is absorbed by the indoor space, 19% by the venetian blind, 12% by the indoor glass, 13% by the outdoor glass, and 38% is reflected away.

The presence of the insect screen reduced the transmitted and reflected solar radiation by about 3% and 10%, respectively. The insect screen also absorbs a noticeable portion of the incident solar radiation. The results in both examples can be checked to confirm that the sum of the absorbed radiation in all of the layers (including the indoor space) plus the reflected radiation is equal to the sum of the incoming beam and diffuse radiation.

CONCLUSIONS

An algorithm has been devised by which beam and diffuse components of solar radiation can be tracked as they interact with a multi-layer system of specular and/or specular/diffuse glazing and shading layers. Analysis results include all beam and diffuse fluxes, providing full detail concerning the quantities of reflected, transmitted, and absorbed radiation—including locations of the absorbed amounts.

This algorithm entails a sequential three-step approach. Edwards' (1977) method is recommended for the beam-beam calculation. An extension of Edwards' method allows for the treatment of shading layers with unequal front and back trans-

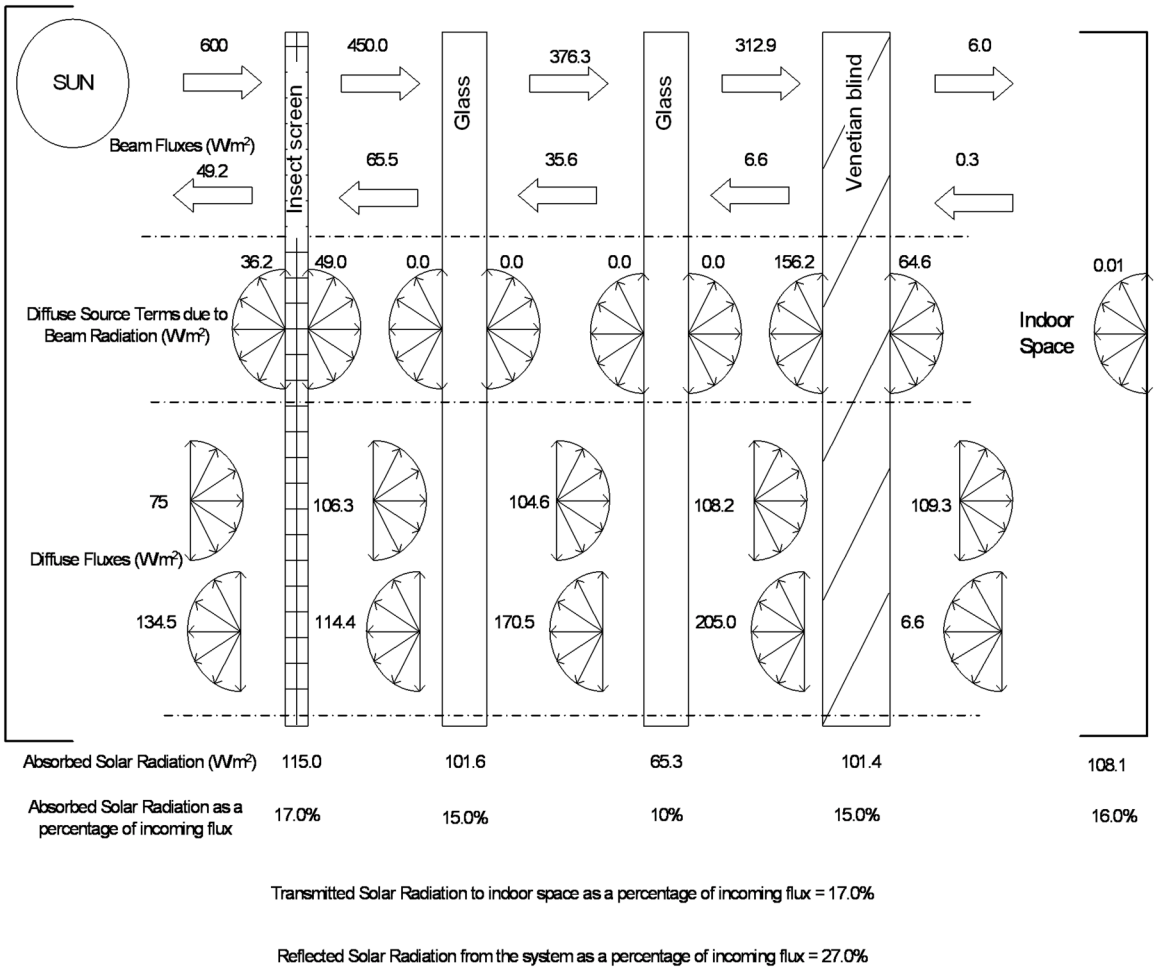

Figure 8 *Sample results: a double-glazed window with a venetian blind on the indoor side and an insect screen on the outdoor side.*

mittance values. The Thomas (1949) algorithm is used in the diffuse-diffuse calculation. The method is sufficiently general to include diffuse incident radiation on the indoor side.

The algorithm has been formulated with computational speed and simplicity as high priorities. Consequently, the resulting computer code is well suited for use within an hour-by-hour building energy analysis.

ACKNOWLEDGMENTS

This research was supported by Natural Sciences and Engineering Research Council (Canada).

REFERENCES

Ames, W.F. 1977. *Numerical Methods for Partial Differential Equations*, 2d ed., p. 52. New York: Academic Press.

Bruce, G.H., D.W. Peaceman, H.H. Rachford, and J.D. Rice. 1953. *Trans. Am. Inst. Min. Engrs (Petrol Div.)* 98:79.

Chantrasrisalai, C., and D.E. Fisher. 2004. Comparative analysis of one-dimensional slat-type blind models. *SimBuild 2004, IBPSA-USA International Conference, Boulder, Colorado.*

Collins, M.E., and S.J. Harrison. 2004. Calorimetric analysis of the solar and thermal performance of windows with interior louvered blinds. *ASHRAE Transactions* 110(1):474–85.

Edwards, D.K. 1977. Solar absorption by each element in an absorber-coverglass array. Technical Note. *Solar Energy* 19:401–402.

Farber, E.A., W.A. Smith, C.W. Pennington, and J.C. Reed. 1963. Theoretical analysis of solar heat gain through insulating glass with inside shading. *ASHRAE Transactions* 69:393–405.

Finlayson, E.U., D.K. Arasteh, C. Huizenga, M.D. Rubin, and M.S. Reilly. 1993. WINDOW 4.0: Documentation of calculation procedures. Energy and Environment Division, Lawrence Berkeley Laboratory, Berkeley, California.

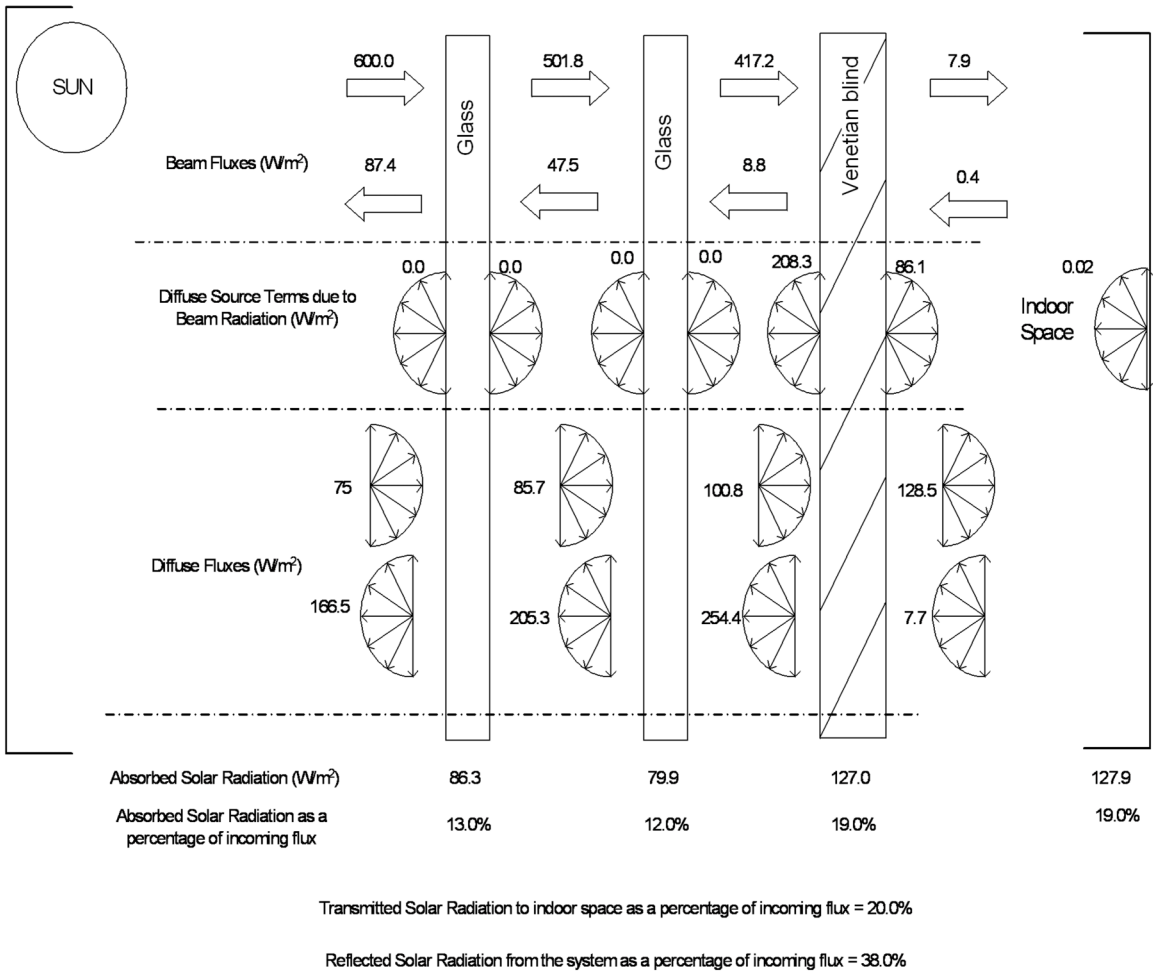

Figure 9 *Sample results: a double-glazed window with a venetian blind on the indoor side.*

Klems, J.H. 1994a. A new method for predicting the solar heat gain of complex fenestration systems—1. Overview and derivation of the matrix layer calculation. *ASHRAE Transactions* 100(1):1065–72.

Klems, J.H. 1994b. A new method for predicting the solar heat gain of complex fenestration systems—2. Detailed description of the matrix layer calculation. *ASHRAE Transactions* 100(1):1073–86.

Klems, J.H., and J.L. Warner. 1995. Measurement of bi-directional optical properties of complex shading devices. *ASHRAE Transactions* 101(1):791–801.

Parmelee, G.V., and W.W. Aubele. 1952. The shading of sun-lit glass: An analysis of the effect of uniformly spaced flat opaque slats. *ASHVE Transactions* 58:377–98.

Pfrommer, P., K.J. Lomas, and C. Kupke. 1996. Solar radiation transport through slat-type blinds: A new model and its application for thermal simulation of buildings. *Solar Energy* 57(2):77–91.

Rheault, S., and E. Bilgen. 1989. Heat transfer analysis in an automated venetian blind system. *Journal of Solar Energy* 111(Feb.):89–95.

Rosenfeld, J.L.J., W.J. Platzer, H. Van Dijk, and A. Maccari. 2000. Modelling the optical and thermal properties of complex glazing: Overview of recent developments. *Solar Energy* 69(Supplement Nos. 1–6):1–13.

Thomas, L.H. 1949. Elliptic problems in linear difference equations over a network. Watson Science Computer Laboratory Report, Columbia University, New York.

UW. 1996. VISION4, Glazing system thermal analysis: Users and reference manuals. Advanced Glazing System Laboratory, University of Waterloo, Ontario.

Wright, J.L., and A. McGowan. 1999. Calculating solar heat gain of window frames. *ASHRAE Transactions* 105(2):1011–21.

Yahoda, D.S., and J.L. Wright. 2005. Methods for calculating the effective solar-optical properties of a venetian blind layer. *ASHRAE Transactions* 111(1):572–86.

APPENDIX A

Edwards' Method,[1] Fortran Subroutine, Arrays Sized for Maximum of *n* = 8

```
      SUBROUTINE EDWRDS(N,RHOF,RHOB,TAUF,
      TAUB,ISOL,QPLUS,QMINUS)
      INTEGER N
      REAL TAUF(8), TAUB(8), RHOF(8), RHOB(8), ISOL
      REAL TED(8), RED(8), QPLUS(8), QMINUS(8)

      RED(1) = RHOF(1)
      TED(1) = 0.0
      DO 1 I=2,N-1
        RED(I) = RHOF(I) + (TAUF(I)* TAUB(I)*RED(I-1)) /
     &                          (1.-(RHOB(I)*RED(I-1)))
        TED(I) = TAUF(I)/(1.-RHOB(I)*RED(I-1))
    1 CONTINUE

      QMINUS(N-1)=ISOL
      QPLUS(N-1)=QMINUS(N-1)*RED(N-1)
      DO 2 I=N-2,1,-1
        QMINUS(I) = QMINUS(I+1)*TED(I+1)
        QPLUS(I) = QMINUS(I)*RED(I)
    2 CONTINUE

      RETURN
      END
```

[1] The code shown here is a modified version of Edwards' (1977) method. The modification makes it possible for layers with unequal front-side and back-side transmittance values to be included in the analysis. The derivation presented by Edwards (1977) applied to layers with $\tau_{f,i} = \tau_{b,i}$, but shading layers, particularly venetian blinds, may not satisfy this restriction when beam-beam properties are considered. The derivation is easily reworked to allow layers with $\tau_{f,bb,i} \neq \tau_{b,bb,i}$.

APPENDIX B

TDMA Solver, Fortran Subroutine, Arrays Sized for Maximum of *m* = 12 (*n* = 8)

```
      SUBROUTINE TDMA(PHI,AP,AE,AW,BP,M)
      REAL PHI(12),AP(12),AE(12),AW(12),BP(12)
      INTEGER J, M
      REAL ALPHA(12), BETA(12)

      ALPHA(1)=AE(1)/AP(1)
      BETA(1) =BP(1)/AP(1)
      DO 1 J=2,M
        ALPHA(J)= AE(J) / ( AP(J)-(ALPHA(J-1)*AW(J)) )
        BETA(J) = ((AW(J)*BETA(J-1)) + BP(J)) /
     &                  ( AP(J)-(ALPHA(J-1)*AW(J)) )
    1 CONTINUE

      PHI(M) = BETA(M)
      DO 2 J=M-1,1,-1
        PHI(J)=( ALPHA(J)*PHI(J+1) ) + BETA(J)
    2 CONTINUE

      RETURN
      END
```

DISCUSSION

Christopher Barry, Director of Technical Services, Pilkington NA, Inc., Toledo, OH: Is the transmission inequality for both directions—as seen with venetian blinds—applicable to surface-treated glass (sand-blasted glass, acid-etched glass)?

John L. Wright: The ability to deal with unequal beam-beam transmission was retained because it is necessary in certain instances, and the venetian blind is presented as an example. This happens because of its asymmetric directional selectivity. This situation doesn't apply to surface-treated glass, so I expect the front and back transmission to be equal in this case.